$RbNb_6Cl_{12}O_2$: CRYSTAL STRUCTURE AND MAGNETIC PROPERTIES

Fakhili Gulo*

Department of Chemistry Education, FKIP - Sriwijaya University
Jl. Palembang-Prabumulih Km 32 Indralaya, OI, Indonesia 30662

Received 17 December 2007; Accepted 4 January 2008

ABSTRACT

A novel niobium oxychloride cluster compound, $RbNb_6Cl_{12}O_2$ was obtained by solid state synthesis from stoichiometric mixture of RbCl, Nb_2O_5, $NbCl_5$ and Nb powder, heated at 675 °C. Its structure was determined by single-crystal X-ray diffraction. It crystallizes in the monoclinic system (a = 6.8097(4) Å, b = 11.6700(9) Å, c = 12.5090(9) Å, ß = 101.337(4) °, V = 974.68(12) Å^3, and Z = 2) with the space group of $P2_1/c$. The cluster framework of this compound is based on $(Nb_6Cl^i_{10}O^i_2)Cl^a_4O^a_2$ units connected via oxide ligands in the a-direction with two Nb–O linkages between adjacent clusters, which resembles intercluster bonding in Chevrel–Sergent phases. In the other two directions, the linkages occur through single Cl^{a-a} bridges. The framework generates channels where the cations Rb^+ are located. This compound contains valence electron concentration (VEC) of 15 per cluster unit and therefore exhibits the paramagnetic behavior.

Keywords: *niobium oxychloride cluster, solid state, VEC, paramagnetic.*

INTRODUCTION

Extended solids containing transition metal clusters have attracted significant interest in applied and fundamental fields of materials research due not only to their remarkable physical and structural properties [1], but also to their potential applications. Indeed, some of these compounds are now well known for their unusual physical properties at high magnetic field or the coexistence of magnetism and superconductivity [2] as well as for their various applications in catalysis process [3] or redox intercalation-desintercalation [4], and their use as precursors for the synthesis of organomineral hybrids by solution chemistry [5].

The most common structural units in these solids are octahedral $(M_6L^i_8)L^a_6$ and $(M_6L^i_{12})L^a_6$ clusters in which the inner ligands (L^i) cap the faces or bridge the edges of the metal octahedron, respectively, and the outer ligands (L^a) are located in the apical positions [6]. One of the most prominent series of cluster compounds are molybdenum chalcogenides with the general formula $A_xMo_6L_8$ (A = Pb, Sn, Cu, Li, La, Eu, etc.; L=S, Se, Te) that known as *Chevrel–Sergent* phases [2, 7]. They are based on a three-dimensional framework of $(M_6L^i_8)L^a_6$ clusters sharing L^a and L^i ligands.

Nb_6 halide and Nb_6 oxide chemistries are now well developed. All these compounds are built from the edge capped $(Nb_6L^i_{12})L^a_6$ units (L^i = inner ligand bridging the edge of the Nb_6 octahedron, L^a = apical ligand on a terminal position). However, important differences between these two classes of compounds exist in their composition and structural characteristics, in relation with the difference between both sizes and formal charges of oxygen and halogen ligands. Indeed, usually in the halide compounds, niobium forms only Nb_6 clusters, while in the oxide ones, isolated niobium and triangular Nb_3 clusters are frequently encountered besides the Nb_6 clusters.

In the Nb_6 halides, the interunit connections are most frequently built by apical ligands shared between adjacent units as in $NaNb_6Cl_{15}$ [8]. This arrangement gives long intercluster distances and, consequently, a strong molecular character remains in these halides leading to insulating behavior. Oppositely, in the Nb_6 oxides the connections between the units involve preferentially inner ligands like in KNb_8O_{14} [9] or $LaNb_7O_{12}$ [10], which give short intercluster distances. In the latter case, the molecular character decreases and a semiconducting behavior is frequently encountered. Between these two classes of compounds, it was interesting to try to obtain Nb_6 oxyhalides with various distributions of chloride and oxide ligands around the cluster in order to favor anisotropic materials.

The first niobium oxychloride cluster compounds were obtained by Perrin and coworkers who investigate these systems with the purpose of decreasing intercluster separation using small oxide ligands [11]. Recently, the preparation and structure of the compound $Na_{0.21}Nb_6Cl_{10.5}O_3$ [12] which is based on octahedral niobium clusters of the $(Nb_6L^i_{12})L^a_6$ type was reported. We have also reported the synthesis and crystal structure of $CsNb_6Cl_{12}O_2$ [13] in which the clusters are strongly bonded in one direction through outer and inner oxide ligands in a way similar to that in *Chevrel–Sergent* phases and $Na_{0.21}Nb_6Cl_{10.5}O_3$, while the linkages in the other two directions occur through outer chloride ligands only. Here, we describe the structure and magnetic properties of a novel niobium oxychloride cluster compound, $RbNb_6Cl_{12}O_2$.

* Corresponding author. Tel/Fax : 0711-580058
Email address : fgulo@unsri.ac.id

EXPERIMENTAL SECTION

Synthesis

The compound, $RbNb_6Cl_{12}O_2$ was synthesized in high-temperature reactions between Nb powders (Ventron, m2N8), $NbCl_5$ (Alfa, 99.9%), Nb_2O_5 (Alfa, 99.5%), and RbCl in the ratio corresponding to stoichiometric mixture. The mixtures were prepared in argon atmosphere, sealed under vacuum in silica tubes, and heated at 675 °C for three days. The $RbNb_6Cl_{12}O_2$ phases were obtained as black crystals. The elemental composition of the products was derived from single crystal X-ray diffraction analysis and confirmed by EDS analyses performed on single crystals.

Crystal X-ray data collection

A suitable single crystal of $RbNb_6Cl_{12}O_2$ was selected and used for structural determination by X-ray diffraction. Intensity data were collected at room temperature by a Nonius KappaCCD diffractometer with MoKα radiation (λ = 0.71073 Å). A crystal-to-detector distance of 25 mm was applied and data collection strategy was performed by using the COLLECT program of KappaCCD software package to measure all the Bragg reflections inside the full sphere until θ = 34.98°. A total of 150 frames were recorded with ΔΦ = 2° rotation scans and Δω = 2° rotation scans to fill the asymmetric unit cell (exposition time = 30 sec./deg.). Finally, 8159 reflections were indexed, Lorentz-polarization corrected and then integrated in the monoclinic symmetry (*p*2 space group) by the DENZO program of the KappaCCD software package.

Structural determination

The extinction conditions indicated $P2_1/n$ as a unique choice of the space group. Initial atomic positions of all atoms were determined by using direct methods [14]. The refinement was carried out with full-matrix least squares methods and Fourier syntheses on F^2 [15]. All the atoms were refined with anisotropic displacement factors. The short distance between the two symmetry-equivalent rubidium positions (1.2494 Å) indicated a partial occupancy of the rubidium sites. The final refinement cycles converged to R_1=0.0628, wR_2=0.0963. Details of data collection and structure refinement are summarized in Table 1. Atomic positions and equivalent isotropic displacement parameters are reported in Table 2. Selected interatomic distances are listed in Table 3. Anisotropic thermal factors and observed and calculated structure factors are available from the authors upon request.

Table 1. Crystal data and structure refinement for $RbNb_6Cl_{12}O_2$.

Formula	$RbNb_6Cl_{12}O_2$
Formula weight	1100.33
Temperature	293(2) K
Wavelength	0.71073 Å
Crystal system	Monoclinic
Space group	$P2_1/c$ No. 14 (choice 2)
Unit cell dimensions	a = 6.8097(4) Å b = 11.6700(9) Å c = 12.5090(9) Å ß = 101.337(4) °
Volume	974.68(12) $Å^3$
Z	2
Density (calculated)	3.749 $g.cm^{-3}$
Absorption coefficient	7.527 mm^{-1}
Crystal size	0.05 x 0.04 x 0.03 mm^3
Theta range for data collection	2.41 to 34.98 °.
Reflections collected	4223
Independent reflections	4223
Reflections observed (>2σ)	2137
Refinement method	Full-matrix least-squares on F^2
Data / restraints / parameters	4223 / 0 / 101
Goodness-of-fit on F^2	1.048
Final R indices [I>2σ(I)]	R_1 = 0.0628, wR_2 = 0.0963
R indices (all data)	R_1 = 0.1697, wR_2 = 0.1224
Largest diff. peak and hole	2.205 and -2.336 $e.Å^{-3}$

Table 2. Atomic coordinates and equivalent isotropic displacement parameters for $RbNb_6Cl_{12}O_2$.

Atom	x	y	z	U(eq) ($Å^2$)
Nb1	0.3385(1)	0.1406(1)	0.4272(1)	0.014(1)
Nb2	0.5558(1)	0.0859(1)	0.6500(1)	0.015(1)
Nb3	0.7701(1)	0.0566(1)	0.4699(1)	0.014(1)
Cl1	0.6224(3)	0.1856(2)	0.8419(2)	0.023(1)
Cl2	0.2602(2)	0.0161(2)	0.7169(1)	0.022(1)
Cl3	0.2498(3)	0.0648(2)	0.2423(2)	0.024(1)
Cl4	0.8657(2)	0.1796(2)	0.6290(2)	0.022(1)
Cl5	0.6334(2)	0.2401(2)	0.3767(2)	0.021(1)
Cl6	0.8761(3)	0.2358(2)	0.0893(2)	0.023(1)
Rb	0.0852(6)	0.0803(4)	0.4588(4)	0.018(1)
O	0.4353(6)	0.0350(3)	0.0093(3)	0.095(2)

Table 3. Selected interatomic distances for $RbNb_6Cl_{12}O_2$.

Nb_6 cluster			
Nb1-Nb2	2.9514(9)	Nb2-Nb3	2.9379(9)
Nb1-Nb2	2.9575(9)	Nb1-Nb1	4.1658(13)
Nb1-Nb3	2.8063(9)	Nb2-Nb2	4.1906(13)
Nb1-Nb3	3.0442(8)	Nb3-Nb3	4.1147(11)
Nb2-Nb3	2.9351(8)		
$[(Nb_6Cl^i_{10}O^i_2)Cl^a_4O^a_2]$ unit			
Nb1-O^i	1.974(4)	Nb2-Cl6	2.457(2)
Nb1-Cl3	2.439(2)	Nb2-Cl1	2.6247(19)
Nb1-Cl5	2.5061(17)	Nb3-O^i	1.993(5)
Nb1-Cl6	2.460(2)	Nb3-O^a	2.195(4)
Nb1-Cl1	2.608(2)	Nb3-Cl2	2.4565(18)
Nb2-Cl2	2.4646(17)	Nb3-Cl4	2.435(2)
Nb2-Cl3	2.441(2)	Nb3-Cl5	2.527(2)
Nb2-Cl4	2.4367(17)		
Rubidium environment			
Rb-Cl1	3.185(4)	Rb-Cl4	3.720(4)
Rb-Cl1	3.246(4)	Rb-Cl6	3.785(4)
Rb-Cl3	3.414(4)	Rb-Cl6	3.871(5)
Rb-Cl5	3.539(4)	Rb-Cl3	4.303(4
Rb-Cl2	3.624(4)	Rb-Cl5	4.567(4)
Rb-Cl2	3.687(4)	Rb-Cl4	4.791(4)
Other short distances			
Nb3-Nb3 intercluster	3.3455(12)	Rb-Nb2	4.478(4)
Nb1-Nb2 intercluster	4.826(1)	"Rb-Rb"	1.257(7)

Magnetic measurements

Magnetic susceptibility measurements for $RbNb_6Cl_{12}O_2$ were carried out at 0.25 kGauss in the temperature range of 5 – 300 K using a superconducting quantum interference device (SQUID) magnetometer. The microcrystalline powders of sample were contained in a gelatin capsule for immersion into the SQUID. No diamagnetic correction was made for the sample container because its signal was insignificant relative to the sample. Diamagnetic correction was calculated for samples from diamagnetism of Rb^+, Cl^-, O^{2-}, and Nb_6 cluster.

RESULT AND DISCUSSION

Niobium oxychloride cluster compound, $RbNb_6Cl_{12}O_2$ is based on an anisotropic three-dimensional framework of interlinked $(Nb_6Cl^i_{10}O^i_2)Cl^a_4O^a_2$ clusters which generates channels where the Rb^+ cations are located (Fig 1.a). The $(Nb_6Cl^i_{10}O^i_2)Cl^a_4O^a_2$ cluster unit (Fig 1.b) is based on Nb_6 octahedron in which all edges are bridged by chloride or oxide ligands (inner ligands, L^i), and six other ligands coordinate to the Nb_6 octahedron in apical positions (outer ligands, L^a).

The oxide ligands are located in two inner positions on opposite sides of the Nb_6 octahedron and in two outer positions that are *trans* to each other. The remaining inner and outer positions are occupied by chloride ligands. This ligand distribution results in an anisotropic cluster unit with symmetry close to C_{2h} (crystallographically imposed symmetry C_i). The Nb–Nb distances for an oxide-bridged edge of the Nb_6 octahedron are 2.8053(10) Å, and those for chloride-bridged edges range from 2.9511(10) to 3.0451(9) Å. All the intraunit distances are in the range of the typical values observed for the niobium oxychlorides cluster compounds [16].

In this niobium oxychloride, the clusters are linked to each other to form a three-dimensional anisotropic framework (Fig 2.a). Each cluster is linked to six neighboring ones by four Cl^{a-a} and two O^{i-a} or O^{a-i} linkages (Fig 2.b). In the *a*-direction, adjacent clusters share two oxide ligands to form one $O^{i–a}$ and one $O^{a–i}$ linkages, similar to intercluster bonding in $Ti_2Nb_6O_{12}$ [17], $Na_{0.21}Nb_6Cl_{10.5}O_3$ [12], and *Chevrel–Sergent* phases [7]. This linkage type leads to a short intercluster Nb–Nb distance of 3.3451(13) Å. In the other directions, adjacent clusters are bridged through one outer chloride ligand. The contrast between the cluster linkages in the *a*-direction and those within the *bc* plane allows for a description of the framework as being formed of chains of oxide-bridged clusters, with outer chloride ligands providing linkages between the chains.

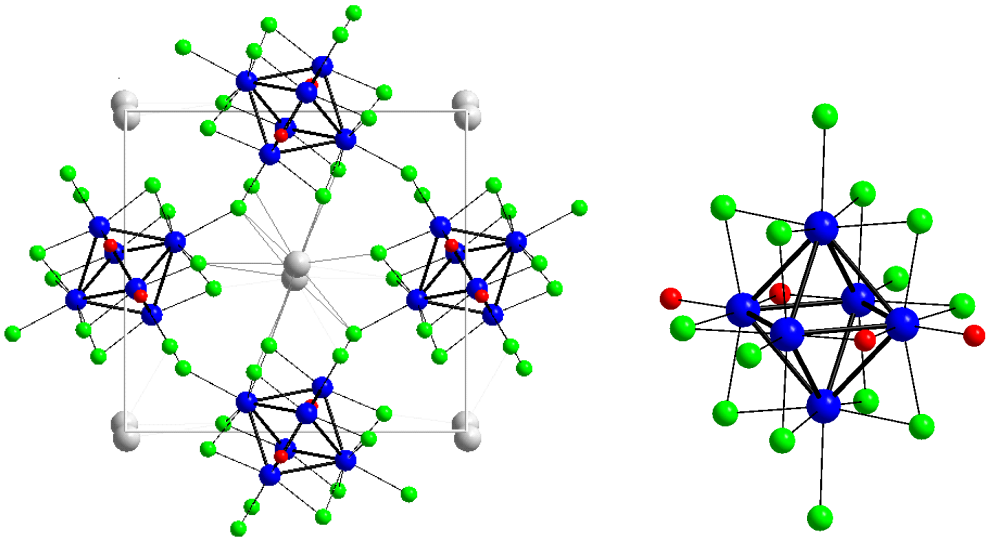

(a) (b)

Fig 1. A view of (a) $RbNb_6Cl_{12}O_2$ structure along the *a*-direction, (b) $(Nb_6Cl^i_{10}O^i_2)Cl^a_4O^a_2$ cluster unit.

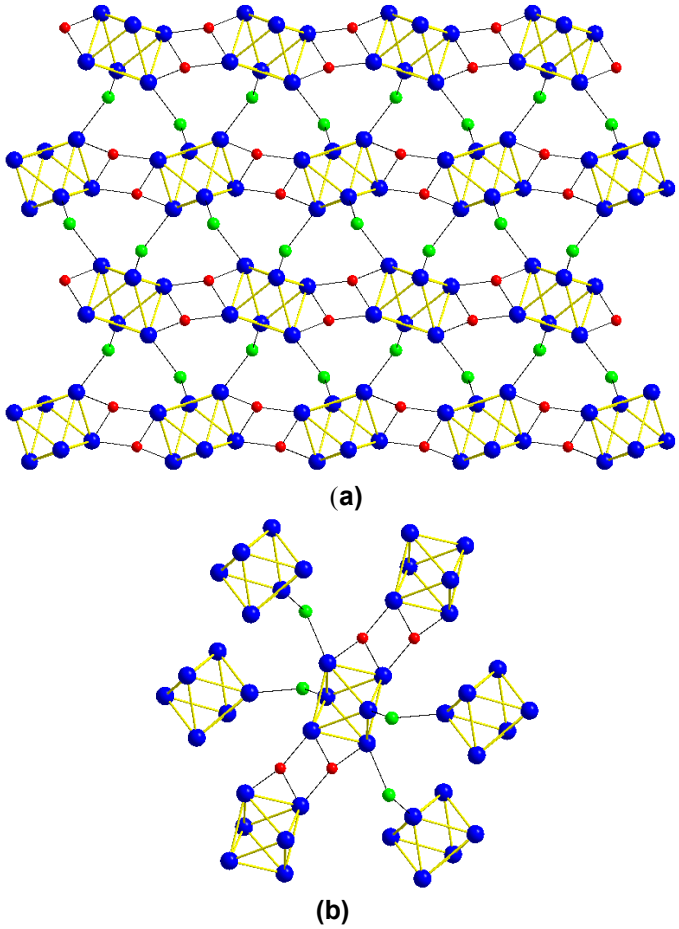

(a)

(b)

Fig 2. (a). A view of the cluster framework in $ANb_6Cl_{12}O_2$ emphasizing the difference of intercluster linkage types between the *a*-direction and *bc* plane. (b). Connection of the Nb_6 cluster with the six adjacent clusters, by $O^{i\text{-}a}$, $O^{a\text{-}i}$ and $Cl^{a\text{-}a}$ ligands.

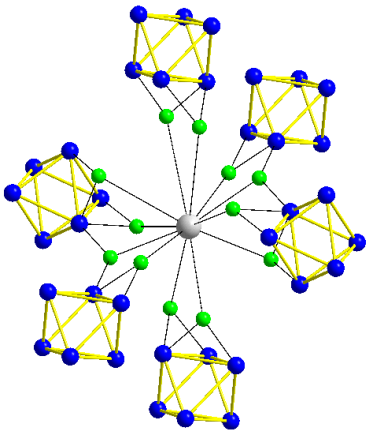

Fig 3. Environment of Rb^+ cations in $RbNb_6Cl_{12}O_2$

The cluster framework generates channels running in the *a*-direction in which the Rb^+ cations are located (Fig 1.a). The Rb sites correspond to vacancies in the distorted close packing of anions that is formed by alternating layers of two types that stack in *[101]*-direction. The anion vacancies layer form elongated cavities that are too large for one and too small for two cations due to the size mismatch between chlorides and oxides ions, results in two closely-spaced partially occupied Rb sites. The separation between two adjacent Rb sites increases as the cation size decreases.

Unusually short A – Cl distances (A = alkali metals) were also found in niobium chloride cluster compounds with fully occupied cationic sites as in the niobium chloride, $K_4Nb_6Cl_{18}$ with K – Cl^a = 2.983 – 3.140 Å [18]. These short A – Cl distances generally correspond to outer chlorides as found in $RbNb_6Cl_{12}O_2$, which is presumably due to higher effective negative charge of outer ligands compared to that of inner ones.

The use of a combination of chloride and oxide ligands has led to a cluster unit with pronounced directional bonding preferences, which resulted in the formation of an anisotropic framework. The framework anisotropy is displayed not only in the strength of Nb–L bonds, but also in the number of these bonds between adjacent clusters in different directions. The high degree of the cluster framework anisotropy is also evidenced by the fact that as the size of A^+ cations increases, the unit cell dimensions increase in the *b*- and *c*- directions and remain constant in the direction of the cluster chains.

The cluster framework of $RbNb_6Cl_{12}O_2$ can also be considered a "dimensional reduction" derivative from the isotropic framework of $Ti_2Nb_6O_{12}$ [17]. Partial substitution of oxide ligands by chlorides and increase of the total number of ligands lead to a transformation from a three-dimensional framework formed by $Nb–O^{a–i}$ and $Nb–O^{i–a}$ linkages to a framework where these linkages extend only in one dimension.

The effect of combining chloride and oxide ligands on the framework topology is also apparent when one compares the cluster frameworks in $RbNb_6Cl_{12}O_2$ to those in Nb_6Cl_{14} [19]. Both framework types have the same number of ligands per cluster and the same connectivity formula, $(Nb_6Cl^i_{10}L^{i-a}_{2/2})Cl^{a-i}_{4/2}L^{a-i}_{2/2}$ (in $RbNb_6Cl_{12}O_2$, L = O; in Nb_6Cl_{14}, L = Cl), however they exhibit different topologies. In both structure-types, two inner and two outer ligands of the cluster are involved in outer–inner and inner–outer linkages, and the remaining four outer ligands participate in outer–outer linkages. The $L^{a–a}$ linkages extend in two dimensions leading to the formation of distorted square-net cluster layers, and $L^{a–i}$ and $L^{i–a}$ linkages connect clusters from adjacent layers. However, in $RbNb_6Cl_{12}O_2$, each cluster is linked to one cluster from adjacent layers via both $O^{i–a}$ and $O^{a–i}$ linkages, while in Nb_6Cl_{14}, each cluster is linked to two clusters from adjacent layers (one $Cl^{a–i}$ linkage to one cluster and one $Cl^{i–a}$ linkage to the other). The differences in the ligand size and the arrangement of $L^{a–i}$ linkages lead to much shorter intercluster distances of 3.3451(13) Å in $RbNb_6Cl_{12}O_2$ compared to 5.07 Å in Nb_6Cl_{14}.

The series of $ANb_6Cl_{12}O_2$ is the first example of an Nb_6 oxychloride with oxide ligands located in outer positions [13]. This difference from other Nb_6 oxychlorides known to date, in all of which oxide ligands occupy inner positions exclusively, could be associated with the absence of a trivalent counterion in $ANb_6Cl_{12}O_2$. The trivalent cations M^{3+} (M=Ti, rare earth metals), which are present in all other Nb_6 oxychlorides, coordinate to all inner oxide ions, increasing the coordination number of oxide ions to three. In the absence of M^{3+} cations, the three-fold coordination of inner oxide ions is achieved by the formation of an additional linkage to a niobium atom from another cluster that can be formally considered as a cation $Nb^{2.5+}$. Similar $O^{i–a}$ linkages leading to three-coordinated oxide ligands are present in the compound $Nb_3Cl_5O_2$ [20], which contains triangular clusters. Thus, the choice between inner or outer position for oxide ions seems to be determined by their preference to occupy sites with larger coordination number.

From the structural data reported in this paper, the valence electron concentration (VEC) per cluster calculated for $RbNb_6Cl_{12}O_2$ is 15. This VEC value is confirmed by the average Nb-Nb intracluster distance that is larger for $ANb_6Cl_{12}O_2$ than for $Cs_2LuNb_6Cl_{17}O$ [21]. Indeed, if we consider only the size effect of O^i on the cluster, we should expect a smaller average Nb-Nb bond length for $RbNb_6Cl_{12}O_2$ with two O^i per unit than for $Cs_2LuNb_6Cl_{17}O$ with only one O^i per unit, but in fact it is the opposite. This feature is easily explained by the predominant effect of the VEC value of 15 in the case of $RbNb_6Cl_{12}O_2$, instead of 16 for $Cs_2LuNb_6Cl_{17}O$. Indeed, this lower VEC value corresponds to a weakening of the Nb-Nb intracluster bonds because one electron is removed from Nb-Nb bonding states, and thus to an increasing of the corresponding bond lengths.

The partial population of the 'a_{2u}' state in $ANb_6Cl_{12}O_2$ is consistent with the trend that the number of valence electrons decreases as the chloride ligands in Nb_6Cl_{18} clusters are progressively substituted by oxygen [22]. The most stable electronic configuration in these clusters is determined by the balance between Nb–Nb bonding and $Nb–L^i$ antibonding contributions to the 'a_{2u}' state. The identity of the outer ligands does not affect the character of the 'a_{2u}' level, because they do not contribute to this state. In niobium chlorides, the 'a_{2u}' state is generally fully occupied, leading to 16 valence electrons per cluster. In the oxides, the stronger $Nb–O^i$ interaction results in an overall antibonding character of the 'a_{2u}' level and a typical VEC of 14.

Most oxychloride cluster compounds with three to six inner oxide ligands have VEC of 14 [16], indicating the dominating influence of the oxide ligands. In contrast, the compound $Cs_2LuNb_6Cl_{17}O$ with one oxide ligand per cluster has VEC of 16 as in most chloride clusters. The cluster unit with two inner oxide ligands, such as that in $RbNb_6Cl_{12}O_2$, represents, probably, an intermediate case in which the addition of electrons to the 'a_{2u}' state neither decreases nor increases the stability of the cluster. This could account for the observed variations in the composition of the title series. Thus, from the electronic point of view, the cluster framework can be expected to be stable with VEC of 14, i.e. without the presence of Rb^+ cations. However, we did not succeed in preparing the ternary $Nb_6Cl_{12}O_2$ by high-temperature techniques, which may imply that the Rb^+ cations are required for the formation of the framework and act as templates.

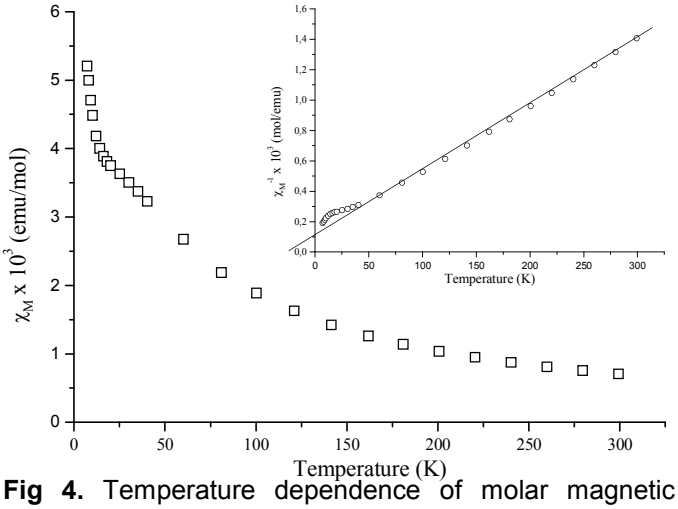

Fig 4. Temperature dependence of molar magnetic susceptibility and inverse molar magnetic susceptibility of $RbNb_6Cl_{12}O_2$

Molar magnetic susceptibility and inverse molar magnetic susceptibility of $RbNb_6Cl_{12}O_2$ as function of temperature are shown in Fig 4. The plot of inverse magnetic susceptibility versus temperature for $RbNb_6Cl_{12}O_2$ shows the presence of linier region in temperature range of 50 – 300 K. The magnetic susceptibility was modeled as a sum of Curie-Weiss and temperature-independent contribution, $\chi(T) = \chi_{TIP} + C/(T-\theta)$ where C is the Curie constant. A linier fit to the above equation leads to an effective magnetic moment of 1.37 μ_B with θ = -25 K.

CONCLUSION

A novel niobium oxychloride cluster compound, $RbNb_6Cl_{12}O_2$ was obtained by solid-state synthesis. The cluster framework is based on $(Nb_6Cl^i_{10}O^i_2)Cl^a_4O^a_2$ clusters connected via oxide ligands in the *a*-direction and chloride ligands in the two other directions. The framework generates channels where the cations Rb^+ are located. This compound contains valence electron concentration of 15 per cluster unit and exhibits a paramagnetic behavior with an effective magnetic moment of 1.37 μ_B.

ACKNOWLEDGEMENT

Author would like to thank Mme C. Perrin for advice and helpful discussions during this work that was partially done at LCSIM Université de Rennes 1, France. Acknowledgments are also addressed to T. Roisnel, Université de Rennes 1 for crystal data collection and R.K. Kremer, Max Planck Institut für Festforschung, Stuttgart, Germany for the magnetic measurements.

REFFERENCES

1. Simon, A., "Discrete and Condensed Transition Metal Clusters in Solids" in *Clusters and Colloids – From Theory to Applications*. Ed. Schmidt, G., VCH Verlagsgesellschaft mbH, Weinheim, 1994, 373 – 458.
2. Fisher, Ø., and Maple, M.P., "Superconducting Ternary Compounds: Prospectsand Perseptives" in *"Topics in Current Physics: Superconductivity in Ternary Compounds.* Eds. Fisher, Ø., and Maple, M.P., Springer-Verlag, Berlin, 1982, 1 – 24.
3. Fischer, C., Alonso-Vante, N., Fiechter, S., and Tributsch, H., 1995, *J. Appl. Electrochem.* 25, 1004.
4. Tarascon, J.M., Di Salvo, F.J., Murphy, D.W., Hull, G.W., Rietman, E.A., and Waszczak, S.V., 1984, *J. Solid State Chem.,* 54, 104.
5. Yaghi, O.M., Scott, M.J., and Holm, R.H., 1992, *Inorg. Chem.,* 31, 4778.
6. Perrin, C., 1997, *J. Alloys Comp.,* 262**,** 10.
7. Chevrel, R., Sergent, M., and Prigent, J., 1971, *J. Solid State Chem.,* **3,** 515.
8. Sägebarth, M. E., Simon, A., Imoto, H., Weppner, W., and Kliche, G., 1995, *Z. Anorg. Allgem. Chem.*, 621, 1589.
9. Köhler, J., Tischtau, R., and Simon, A., 1991, *J. Chem. Soc., Dalton Trans*., 829.
10. Xu, J., Emge, T., and Greenblatt, M., 1996, *J. Solid State Chem*., 123, 21.
11. Cordier, S., Gulo, F., and Perrin, C., 1999, *Solid State Sci.,* 1**,** 637.
12. Gulo, F. and Perrin, C., 2002, *J. Solid State Chem,* 163, 325.
13. Gulo, F. and Perrin, C., 2000, *J. Mater. Chem.* 10, 1721.
14. Sheldrick, G.M., 1997, *SHELXS-97, Crystal Structure Solution*, University of Göttingen.
15. Sheldrick, G.M., 1997, *SHELXL-97, Crystal Structure Refinement*, University of Göttingen.
16. Naumov, N.G., Cordier, S., Gulo, F., Roisnel, T., Fedorov, V.E., and Perrin, C., 2003, *Inorg. Chim. Acta,* 350, 503.
17. Anokhina, E.V., Essig, M.W., Day, C.S., and Lachgar, A., 1999, *J. Am. Chem. Soc.,* 121**,** 6827.
18. Simon, A., von Schnering, H.-G., and Schäfer, H., 1968, *Z. Allg. Anorg. Chem.,* 361**,** 235.
19. Simon, A., von Schnering, H.-G., Wöhrle, H., and Schäfer, H., 1965, *Z. Allg. Anorg. Chem.,* 339, 155.
20. Gulo, F. and Perrin, C., 2000, *Mater. Res. Bull.,* 35**,** 253.
21. Cordier, S., Perrin, C., and Sergent, M., 1996, *Mat. Res. Bull.,* 31, 683.
22. Ogliaro, F., Cordier, S., Halet, J.F, Perrin, C., Saillard, J.Y., and Sergent, M., 1998, *Inorg. Chem.,* 37, 6199.